Shroom2 regulates contractility to control endothelial morphogenesis

Matthew J. Farber, Ryan Rizaldy, and Jeffrey D. Hildebrand
Department of Biological Sciences, University of Pittsburgh, Pittsburgh, PA 15260

ABSTRACT **The intrinsic contractile, migratory, and adhesive properties of endothelial cells are central determinants in the formation of vascular networks seen in vertebrate organisms. Because Shroom2 (Shrm2) is expressed within the endothelium, is localized to cortical actin and cell–cell adhesions, and contains a conserved Rho kinase (Rock) binding domain, we hypothesized that Shrm2 may participate in the regulation of endothelial cell behavior during vascular morphogenesis. Consistent with this hypothesis, depletion of Shrm2 results in elevated branching and sprouting angiogenic behavior of endothelial cells. This is recapitulated in human umbilical vein endothelial cells and in a vasculogenesis assay in which differentiated embryonic stem cells depleted for Shrm2 form a more highly branched endothelial network. Further analyses indicate that the altered behavior observed following Shrm2 depletion is due to aberrant cell contractility, as evidenced by decreased stress fiber organization and collagen contraction with an increase in cellular migration. Because Shrm2 directly interacts with Rock, and Shrm2 knockdown results in the loss of Rock and activated myosin II from sites of cell–cell adhesion, we conclude that Shrm2 facilitates the formation of a contractile network within endothelial cells, the loss of which leads to an increase in endothelial sprouting, migration, and angiogenesis.**

Monitoring Editor
Mark H. Ginsberg
University of California, San Diego

Received: Jun 11, 2010
Revised: Dec 6, 2010
Accepted: Jan 6, 2011

INTRODUCTION

Shroom3 (Shrm3) has been shown to be a critical regulator of cell morphology in several cellular contexts and animal model systems (Hildebrand and Soriano, 1999; Hildebrand, 2005; Haigo *et al.*, 2003; Lee *et al.*, 2007; Nishimura and Takeichi, 2008; Taylor *et al.*, 2008; Chung *et al.*, 2010). Shrm3-mediated morphogenesis is dependent on its ability to bind both F-actin and Rho kinase (Rock) (Hildebrand, 2005; Nishimura and Takeichi, 2008). It is predicted that actin binding targets Shrm3 to the tight junction in polarized epithelia. Shrm3 can then recruit Rock to the tight junction, resulting in the localized activation of nonmuscle myosin II (myosin II) and subsequent apical constriction (Hildebrand, 2005; Nishimura and Takeichi, 2008). In addition to the ability to regulate actomyosin networks, Shrm3 has been implicated in regulating the apical positioning of γ-tubulin and subsequent microtubule organization in *Xenopus* epithelial cells (Lee *et al.*, 2007). It is unclear whether these two activities of Shrm3 are directly related or occur independently. In vertebrates, the Shroom proteins contain another family member, Shrm2, which shares several structural and functional characteristics with Shrm3. Like Shrm3, Shrm2 contains an N-terminal postsynaptic density 95/disc-large/zona occludens (PDZ) domain of unknown function; a centrally located, conserved actin binding module centered on the Shroom domain 1 (SD1); and a C-terminally located SD2, which, in the case of Shrm3, directly binds to Rock (Nishimura and Takeichi, 2008). Unlike Shrm3, Shrm2 does not induce apical constriction in either *Xenopus* ectodermal epithelium (Fairbank *et al.*, 2006) or cultured Madin-Darby canine kidney (MDCK) epithelial cells (Dietz *et al.*, 2006). However, Shrm2 has been shown to control other aspects of morphogenesis in *Xenopus* embryos, such as epithelial thickening and pigment accumulation (Fairbank *et al.*, 2006; Lee *et al.*, 2009).

This article was published online ahead of print in MBoC in Press (http://www.molbiolcell.org/cgi/doi/10.1091/mbc.E10-06-0505) on January 19, 2011.

Address correspondence to: Jeffrey D. Hildebrand (jeffh@pitt.edu).

Abbreviations used: aa, amino acid; E, embryonic day; ES, embryonic stem; FA, focal adhesion; FAK, focal adhesion kinase; FBS, fetal bovine serum; GFP, green fluorescent protein; GST, glutathione *S*-transferase; HUVEC, human umbilical vein endothelial cell; IPTG, isopropyl β-D-1-thiogalactopyranoside; MDCK, Madin-Darby canine kidney; MLC2, myosin light chain 2; MYPT1, myosin phosphatase 1; PDZ, postsynaptic density 95/disc-large/zona occludens; PECAM-1, platelet endothelial cell adhesion molecule 1; PFA, paraformaldehyde; pMLC, monophosphorylated MLC; ppMLC, diphosphorylated MLC; RNAi, RNA interference; Rock, Rho kinase; SBD, Shroom binding domain; SD1, Shroom domain 1; shRNA, short-hairpin RNA; siRNA, small interfering RNA; SPR, serine/proline-rich region; VEGF, vascular endothelial growth factor.

In mice, Shrm2 is highly expressed in various populations of polarized epithelial cells, including the neural epithelium, gut, eye, lung, and kidney. Additionally, Shrm2 is highly expressed in the endothelium of the developing vasculature (Dietz *et al.*, 2006). This is consistent with the other cell types that express Shrm2, as the endothelium itself is a polarized population of epithelia. Endothelial cells exhibit the remarkable capacity to undergo dramatic changes in morphology and migration in order to form the network of tubes that are seen in the embryo during and after vasculogenesis. Initial formation and subsequent remodeling of the vascular network are dependant on both the ability of endothelial cells to sprout new branches via the formation of filopodia and migration to new positions in the network (De Smet *et al.*, 2009). One of the critical determinants of the migratory behavior of endothelial cells is myosin II contractility downstream of Rock. It has been demonstrated that inhibition of myosin II or Rock results in increased endothelial sprouting, suggesting that this pathway is a critical regulator of vascular architecture (Mavria *et al.*, 2006; Abraham *et al.*, 2009; Fischer *et al.*, 2009; Kroll *et al.*, 2009). In this context the function of Rock seems to negatively regulate membrane protrusion and cell migration at the level of cortical contractility. Specifically, a Rock–myosin II network induces cortical tension that is proposed to inhibit the ability of cells to form membrane protrusions and migrate. This is supported by the observation that localized addition of pharmacological inhibitors of this pathway results in the rapid formation of endothelial filopodial outgrowth followed by cell migration (Fischer *et al.*, 2009).

In this study we have investigated the function of Shrm2 as a potential regulator of the cellular and angiogenic behavior of endothelial cells. On the basis of previous work, we hypothesized that Shrm2 might regulate these biological processes via Rock localization, impacting subsequent contractility. Using small interfering RNA (siRNA) and short-hairpin RNA (shRNA) approaches in both established endothelial cells and in primary endothelia derived from mouse embryonic stem (ES) cells, we show that depletion of Shrm2 results in increased angiogenesis due to decreased cellular contractility. This decrease in contractility appears to result from diminished Rock and myosin II activity at the cell cortex and the disorganization of the actin cytoskeleton. These alterations in cellular architecture cause increases in cell protrusions and alter cellular migration. Together, these data indicate that Shrm2 is a vital regulator of endothelial cell behavior during vascular morphogenesis. Additionally, our findings expand the inclusion of the Shroom–Rock complex in multiple cellular processes and suggest that this conserved signaling complex may be utilized in a variety of biological events that require Rock activity.

RESULTS

Knockdown of Shroom2 increases sprouting in angiogenesis and vasculogenesis assays

Previous studies from our lab have described the expression and localization of Shrm2 in the developing vasculature of mouse embryos and the C166 endothelial cell line (Dietz *et al.*, 2006). Because C166 cells are derived from the murine yolk sac (Wang *et al.*, 1996), we sought to confirm endogenous expression and localization of Shrm2 in the yolk sac in vivo. Staining of yolk sacs of embryonic day (E) 9.5 embryos to detect both Shrm2 and platelet endothelial cell adhesion molecule 1 (PECAM-1), an endothelial-specific adhesion protein, shows that Shrm2 is expressed throughout the yolk sac vasculature in both large vessels (Figure 1A) and the capillary plexus (Figure 1B). In addition, the Shrm2 protein is enriched at sites of cell–cell adhesion, similar to what is seen in the embryo proper and in C166 cells. On the basis of these data and those from other published works (Wang *et al.*, 1996; Zhou *et al.*, 2004), we conclude that C166 cells are a viable cell type to explore the function of Shrm2 in endothelial cell behavior. Therefore we utilized siRNA to knock down the expression of Shrm2 in these cells. C166 cells treated with a control nontargeting siRNA (siControl) form a confluent monolayer and exhibit Shrm2 and ZO1 distribution at cell–cell junctions (Figure 1C). Cells treated with Shrm2-specific siRNA (siShrm2) also form confluent monolayers with no appreciable change in adherens junctions or tight junctions, but Shrm2 staining is virtually eliminated from the majority of these cells (Figure 1D and Supplemental Figure S1). Consistent with the immunostaining results, Western blotting shows that Shrm2 protein is reduced by ~70% using two different siRNAs, one targeting the 3′ untranslated region (siShrm2–7) and the other targeting the coding sequence (siShrm2–8) of the Shrm2 mRNA (Figure 1E). Treatment of cells with siRNA did not alter the rates of proliferation (unpublished data), and all results have been verified using both Shrm2 siRNAs, but data are typically shown from experiments using siShrm2–8. Because we obtain similar results using two different siRNAs that target unique regions of the *Shrm2* transcript, we are confident that the observed phenotypes result from specific depletion of Shrm2 protein.

One hallmark of endothelial cells is their ability to form a capillary network when cultured on matrigel. Control C166 cells form a multicellular vascular network when grown under these conditions (Figure 1F). This multicellular network is most morphologically similar to the large vessels of the yolk sac and the early vessels formed by embryoid bodies (Figure 1A and Supplemental Figure S2). To test the role of Shrm2 in this endothelial behavior, siShrm2 C166 cells were plated on matrigel and allowed to undergo angiogenesis. Under these conditions we observe that siShrm2 C166 cells have elevated branching capacity (Figure 1, G and H). While treatment with both siShrm2–7 and siShrm2–8 yields a more highly branched network, C166 cells with the greatest degree of knockdown (siShrm2–8) show areas that have failed to undergo tubulogenesis (Figure 1H, arrow). Similar outcomes have been seen with a broad Rock inhibitor, Y27632, such that angiogenesis is inhibited in both C166 cells (unpublished data) and bovine retinal endothelial cells (Bryan *et al.*, 2010). Because Shrm2-deficient endothelial cells form a more branched network on matrigel, we wanted to further investigate and validate the effect of Shrm2 loss using an in-gel sprouting angiogenesis assay. Control siRNA and siShrm2 spheroids of equal cell number were embedded in collagen gels, cultured for 48 h, and then analyzed for the extent of sprouting. Consistent with the matrigel angiogenesis assay, siShrm2 cells demonstrated significantly elevated sprouting compared with control cells (Figure 1, I–K). To verify these results in a primary cell line, we confirmed expression of hShrm2 in primary human umbilical vein endothelial cells (HUVECs) (Figure 1L). After transfection with hShrm2 siRNA, Shrm2 protein is reduced by ~75% (Figure 1L). Similar to C166 cells, Shrm2 knockdown in HUVECs increases branching during matrigel angiogenesis (Figure 1, M and N).

While Shrm2 knockdown in both C166 cells and HUVECs leads to an increase in branching, these cell types form morphologically distinct networks on matrigel. C166 cells form large multicellular cords, while HUVECs form a single cellular capillary-like network (Supplemental Figure S2, A–C). Thus we sought to determine the effect of Shrm2 knockdown in a model more similar to C166 cells and the vascular network observed in the yolk sac and embryo during development. Because C166 cells are derived from the yolk sac where initial vasculogenesis occurs, we used a vasculogenesis assay

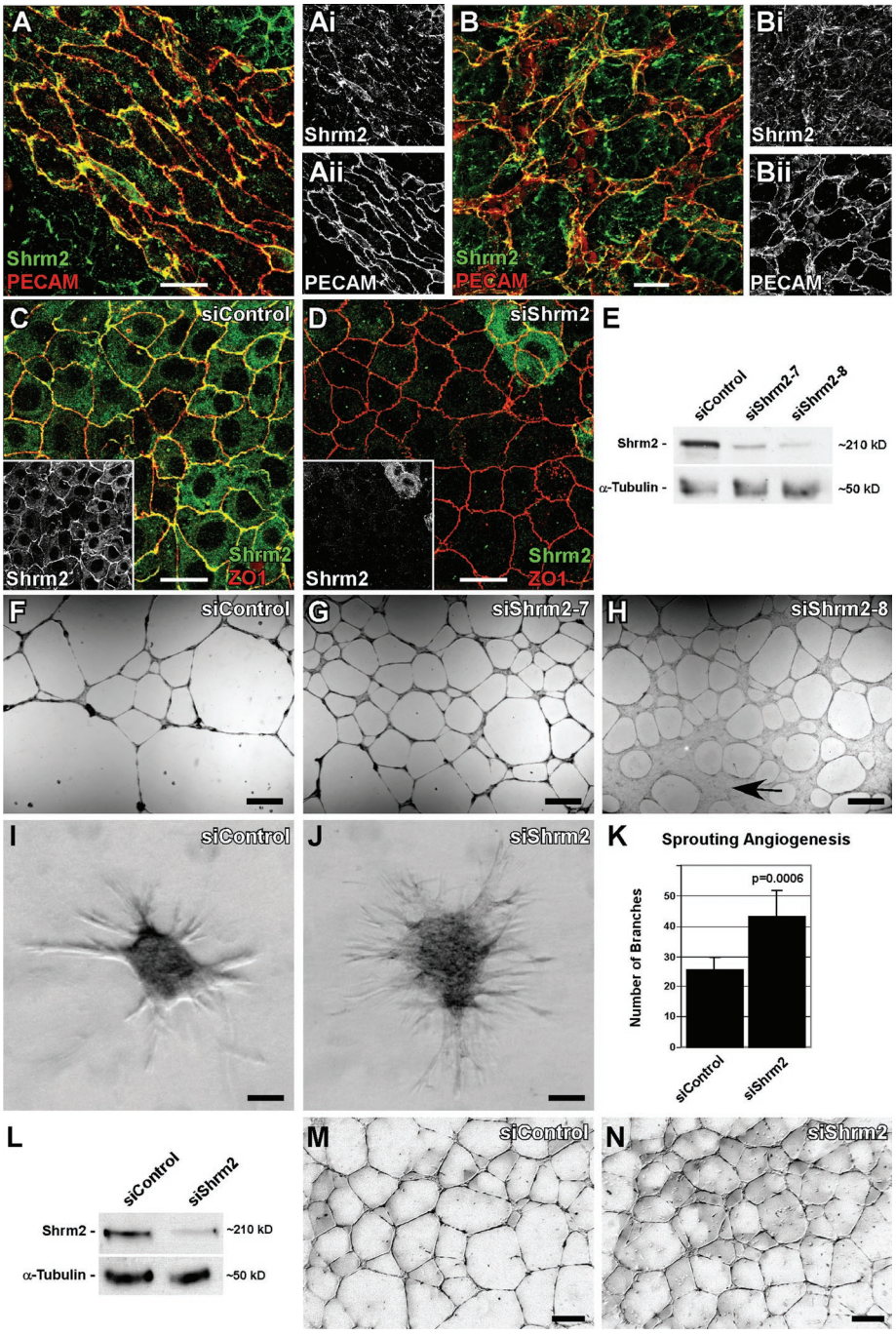

FIGURE 1: Shrm2 knockdown stimulates endothelial angiogenesis. (A and B) Murine yolk sacs at E9.5 stained with PECAM and Shrm2 antibodies show Shrm2 localization at cellular junctions in both large vessels (A) and the capillary plexus (B). (C and D) C166 endothelial cells were treated with a nontargeting siRNA (siControl) (C) or a Shrm2-specific siRNA (siShrm2) (D) and were stained with Shrm2 (inset) and ZO1. (E) Shrm2 knockdown from two different siRNAs was confirmed via Western blot. α-Tubulin was used as a loading control. (F–H) siControl (F), siShrm2–7 (G), or siShrm2–8 (H)–treated C166 cells were plated on matrigel to examine angiogenic potential. Arrow indicates an area that has failed to undergo angiogenesis. (I–K) siControl (I) and siShrm2 (J) C166 cells were grown as spheroids for use in a collagen sprouting angiogenesis assay. Quantification of collagen sprouting angiogenesis is shown in (K). The numbers of branch tips are represented as the mean ± SD (n = 7 spheroids). (L) Western blot of Shrm2 knockdown in HUVECs. (M and N) Matrigel angiogenesis assay for siControl (M) and siShrm2 (N)–treated HUVECs. Scale bars = 25 μm in A–D; 1 mm in F–H; 125 μm in I, J, M, and N.

in which ES cells can be differentiated into a multicellular branching endothelium (Kappas and Bautch, 2007). It should be noted that ES cells express Shrm2 endogenously (Figure 2Ai). To address the role of Shrm2 in endothelial cells derived from ES cells, we generated cell lines that stably express Shrm2-specific shRNAs. Shrm2 knockdown was confirmed via both immunofluorescence staining (Figure 2, Ai and Bi) and Western blot (Figure 2C). Stable ES cells were then grown in suspension to form embryoid bodies, allowed to reattach to tissue culture dishes, and grown for 9–11 d in differentiation media. Differentiated cultures were fixed and immunostained to visualize the vasculature. Consistent with the results obtained using C166 cells and HUVECs, shShrm2 ES cells generate hyperbranched endothelial networks when compared with vector control ES cells (Figure 2, D and E). When observed at higher magnification, the control vasculature exhibits uniform cell borders and few filopodial extensions (Figure 2Di). In stark contrast, the Shrm2-deficient vasculature exhibits a plethora of filopodia-like extensions (Figure 2Ei). Shrm2 remains efficiently knocked down after differentiation (Supplemental Figure S1, F and G). Together these experiments suggest that, within the endothelium, Shrm2 is involved in negatively regulating vessel branching and that this may be controlled at the level of the cytoskeleton.

Shroom2 regulates endothelial contractility through interaction with Rock

Several studies have previously shown that reduced Rock activity and myosin contractility correlates with both increased angiogenesis and increased filopodia formation in endothelial cells (Mavria *et al.*, 2006; Fischer *et al.*, 2009; Kroll *et al.*, 2009). Along these lines, Shrm2 contains the conserved SD2 motif that has been shown to mediate a direct interaction between Shrm3 and Rock and between *Drosophila* Shroom and *Drosophila* Rho-associated kinase to facilitate apical constriction (Dietz *et al.*, 2006; Nishimura and Takeichi, 2008; Bolinger *et al.*, 2010). On the basis of these observations, we hypothesized that the increase in sprouting observed from Shrm2 knockdown is due to loss of Rock-mediated contractility. To test this hypothesis, we first verified an interaction between Rock and Shrm2. In glutathione *S*-transferase (GST) pull-down experiments, the Shroom binding domain (SBD) of hRock1 interacts with Shrm2, and the Shrm2 SD2 domain interacts with endogenous Rock1 and Rock2 (Figure 3A and Supplemental Figure S3A). In addition, the Shrm2 SD2 domain and the hRock1 SBD domain can be copurified when expressed together in bacteria (Supplemental Figure S3B). This is a specific interaction, as the actin binding domain (SD1) of Shrm2 does not pull down the Rock SBD (unpublished data). In C166 cells grown on coverslips, we can

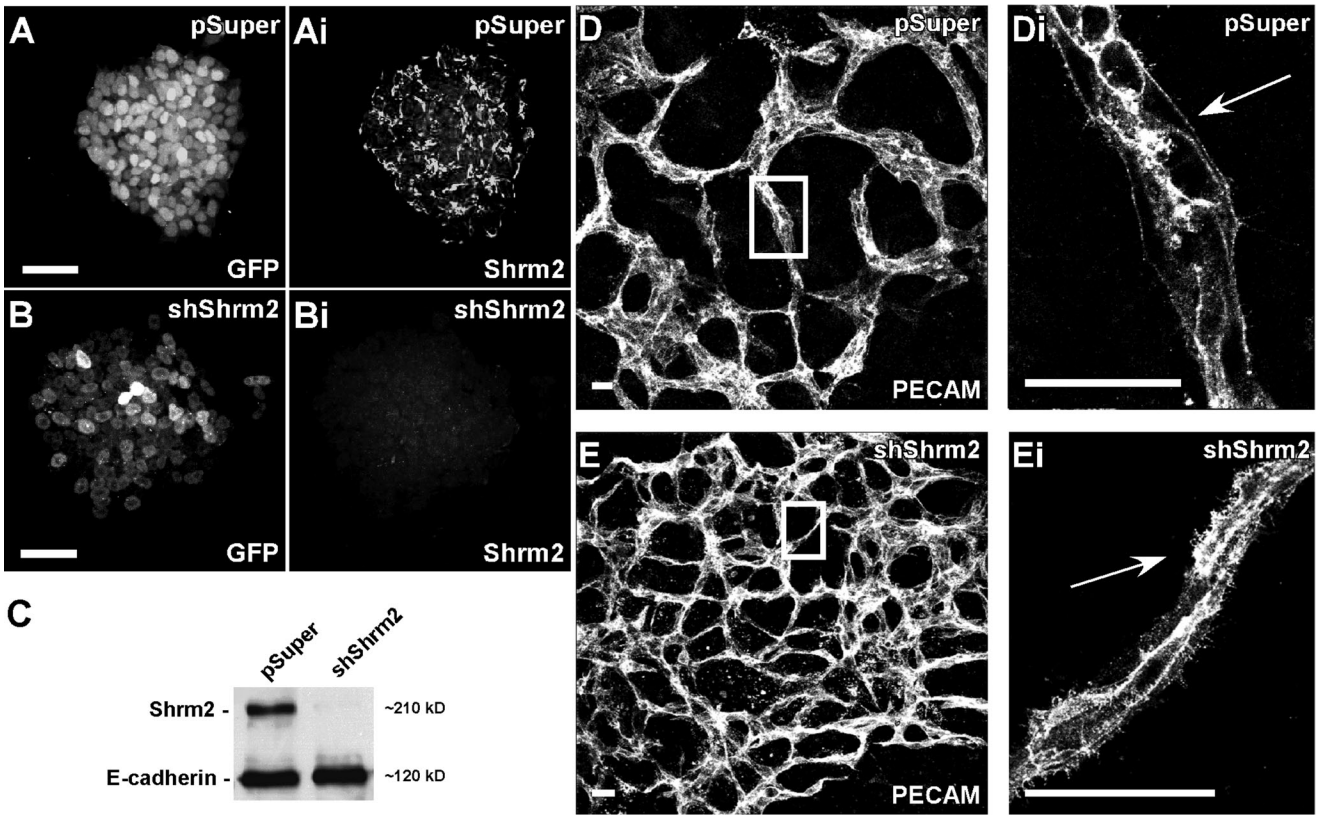

FIGURE 2: Stable knockdown of Shrm2 in murine ES cells enhances vasculogenesis. (A–C) ES cells stably transfected with the parental vector pSuper-GFPneo^r (pSuper) (A) or pSuper-shShrm2 (shShrm2) (B) were stained to detect GFP and Shrm2. Stable knockdown was confirmed by Western blotting (C). E-cadherin was used as a loading control. (D and E) After differentiation, pSuper (D) and shShrm2 (E) cells were stained with PECAM to visualize the resulting endothelial network. Boxed regions in D and E are enlarged in Di and Ei. While distinct boundaries exist between control endothelial and surrounding cells (Di), numerous filopodia-like extensions are found throughout the Shrm2-deficient endothelium (Ei) (compare arrows). Scale bars = 25 μm in A and B; 100 μm in D and E.

visualize sparse Rock1 at cell–cell junctions as indicated by colocalization with ZO1 (Figure 3B). Importantly, this localization appears to be dependent on Shrm2, as this population of Rock is lost in siShrm2 C166 cells (Figure 3C). Knockdown of Shrm2 has no effect on Rock expression as indicated by Western blot (Supplemental Figure S3C). Shrm2 recruitment of Rock is also observed in MDCK cells engineered to express Shrm2 following withdrawal of doxycycline. In the presence of doxycycline, no Shrm2 is detected and no Rock is observed at tight junctions (Supplemental Figure S3D). After Shrm2 induction, both Shrm2 and Rock colocalize at tight junctions (Supplemental Figure S3E). These data indicate that Shrm2 can directly bind Rock in vitro and regulate its subcellular distribution in vivo.

It has been speculated that Shrm proteins can regulate cell and tissue morphology by controlling myosin II–dependent contraction. On the basis of this notion and the above results, we hypothesized that if Shrm2 is involved in localizing Rock to cell–cell junctions, then it may play a role in establishing endothelial contractility. To test this, we analyzed the ability of Shrm2-deficient cells to contract collagen gels. Control and siShrm2 C166 cells were plated on a bed of collagen attached to the well and allowed to form a confluent monolayer. Following monolayer formation, the mechanically loaded gels were detached from the gel and allowed to contract for 6 h. Quantification shows that Shrm2-deficient cells are not able to contract the collagen gel to the same extent as control cells (Figure 3D). Collagen gel contraction is also dependent upon Rock, as treatment of control cells with Rock inhibitor contracted gels to a lesser extent. Interestingly, Shrm2-deficient endothelial cells are more sensitive to Rock inhibition and contract the gel less than the inhibitor or siShrm2 alone. We predict that this sensitivity is due to an interaction between Shrm2 and Rock, which helps establish endothelial contractility. These results document for the first time that Shrm proteins can indeed control the contractile properties of a population of polarized cells.

Activated Rock is thought to cause myosin II contraction by directly phosphorylating the regulatory myosin light chain 2 (MLC2) (Amano *et al.*, 1996) and inhibiting the targeting subunit of myosin phosphatase 1 (MYPT) (Kimura *et al.*, 1996). Rock may also influence contractility by regulating actin dynamics through activation of LIM kinase and subsequent cofilin phosphorylation (Maekawa *et al.*, 1999). To determine whether Shrm2 knockdown affects Rock activity, we examined the phosphorylation state of several downstream Rock effectors. Interestingly, while monophosphorylated MLC2 (pMLC) is unaffected, diphosphorylated MLC2 (ppMLC) levels are reduced 50% in siShrm2 C166 cells (Figure 3E). These results suggest that loss of Shrm2 leads to a loss of Rock activity. A similar role for Rock in the regulation of ppMLC2 but not pMLC2 has been observed in MDCK cells (Watanabe *et al.*, 2007). Additional Rock effectors, MYPT and FAK (Le Boeuf *et al.*, 2006), show reduced phosphorylation by ~25% while p-cofilin levels remain unchanged (Figure 3E). These observations suggest that the Shrm2–Rock complex could be working at the level of myosin II activity to control actin organization. To address this issue, control and siShrm2 cells were stained to detect ppMLC2 at cell–cell junctions (apical) and stress fibers (Figure 3, F–I). In control cells ppMLC can be detected at both of

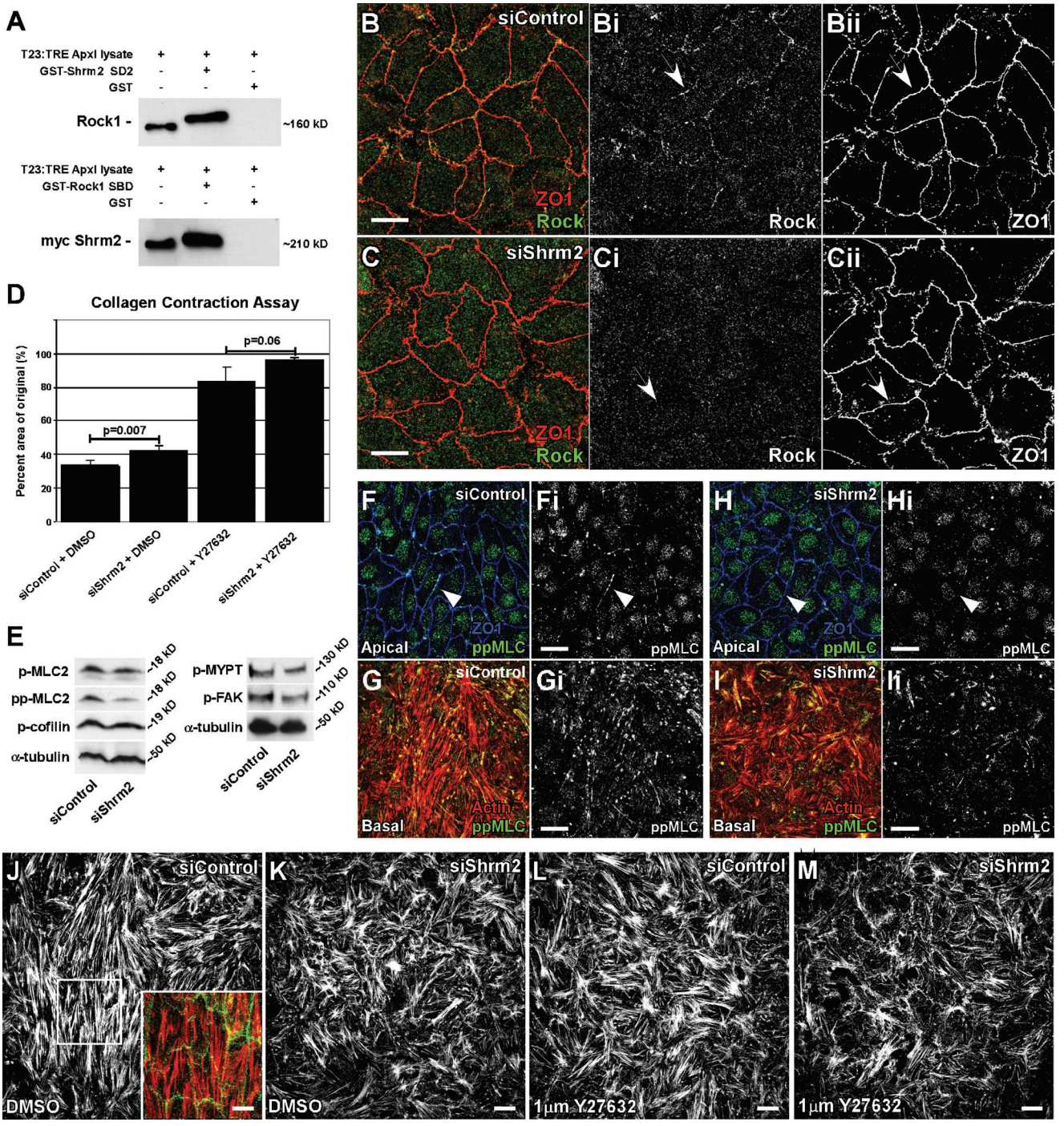

FIGURE 3: Shrm2 interacts with Rock and promotes endothelial contractility. (A) A GST-tagged mShrm2 SD2 or a GST-tagged Shroom binding domain (SBD) of hRock1 were incubated with total cell lysate from T23 cells engineered to express myc-Shrm2 under the tetracycline response element promoter. Following GST pull down, the Shrm2 SD2 interacts with endogenous Rock1, and the Rock1 SBD interacts with full-length myc-Shrm2. (B and C) siControl (B) or siShrm2 (C) C166 cells were stained with Rock1 (Bi and Ci) and ZO1 (Bii and Cii) antibodies. Arrows indicate loss of Rock localization to tight junctions after Shrm2 knockdown. (D) Contractility of siControl or siShrm2 cells with or without the Rock inhibitor Y27632 was assessed through the ability of a monolayer to contract a collagen gel. Quantification is graphed as the percentage of area of the original after 4 h, represented by the mean ± SD (n = 3). (E) Phosphorylation of Rock effectors was visualized by Western blotting. α-Tubulin was used as a loading control. Representative blots from three independent experiments are shown. p-MLC2, phospho-myosin light chain 2 (Ser-19); pp-MLC2, diphospho-myosin light chain 2 (Thr-18/Ser-19); p-MYPT, phospho-myosin phosphatase binding subunit 1 (Thr-696); pFAK, phospho-focal adhesion kinase (Tyr-397). (F–I) Control (F and G) and Shrm2 knockdown (H and I) C166 cells were stained for ppMLC (Fi–Ii) and either ZO1 (F and H) or actin (G and I). Loss of Shrm2 leads to loss of pp-MLC2 at both stress fibers and cell–cell junctions (compare arrowheads). (J–M) Stress fiber organization was examined by immunostaining for actin in C166 cells treated with siControl (J), siShrm2 (K), siControl and Y27632 (L), and siShrm2 and Y27632 (M). Inset is a merge for apical Shrm2 (green) and basal stress fibers (red). Scale bars = 25 μm.

these subcellular locations (Figure 3, Fi and Gi). In contrast, the staining in cell–cell junctions is largely lost and the stress fiber staining is both reduced and disorganized in the siShrm2 cells (Figure 3, Hi and Ii). On the basis of these results, we suggest Shrm2 works to control endothelial contractility via the localized activation of actomyosin.

Because Rock activity and myosin II contractility have been shown to play a significant role in the formation and organization of actin stress fibers (Ishizaki *et al.*, 1997; Uehata *et al.*, 1997), we examined stress fibers in siShrm2 C166 cells. In control cells, stress fibers are typically arranged in thick bundles that are aligned parallel to each other within the cell and appear to be contiguous with bundles in adjacent cells (Figure 3J, inset); a similar organization has been observed in HUVEC endothelial cells (Millán *et al.*, 2010). This organization is lost in siShrm2 cells, as stress fibers appear randomly oriented (Figure 3K). A similar change in stress fiber organization can be found in control C166 cells treated with a low concentration of Rock inhibitor (1 μM) (Figure 3L). Consistent with the idea that Shrm2 and Rock work together to control cell morphology, stress fibers are greatly diminished and further disorganized in siShrm2 cells that are treated with 1 μM Rock inhibitor (Figure 3M). Because Shrm2 is not detected at focal adhesions (FAs), a major regulator of stress fibers, yet we see changes in stress fiber organization and reduced pFAK levels after Shrm2 knockdown, we deduce that these changes occur indirectly through the reduction of cortical contractility.

The loss of Shroom2 influences endothelial migration

Rock activity can enhance or inhibit cellular migration depending on the particular cell type (reviewed in Riento and Ridley, 2003). To observe the effect of Shrm2 knockdown and concomitant loss of endothelial contractility on C166 migration, we subjected siShrm2 C166 cells to a scratch wound assay. Loss of Shrm2 significantly increases migration of C166 cells into the wound relative to control cells (Figure 4A). siShrm2 cells completely closed the wounds by 24 h while control wounds were ~90% closed at this time (Figure 4B). To confirm these results, migration was also assessed using a Boyden chamber. Consistent with the above wound-closing assay, siShrm2 cells demonstrate a significant increase in migration in comparison to control cells (Figure 4C). We next examined the effects of Rock inhibition on C166 migration. Rock inhibition enhances migration in both a scratch wound (Figure 4A) and Boyden chamber assay (Figure 4C). In the presence of mild Rock inhibition, Shrm2-deficient cells migrate more quickly than with Rock inhibition or siShrm2 alone. The opposite has been observed in HUVEC cells, where Rock inhibition attenuates vascular endothelial growth factor (VEGF)–stimulated migration (van Nieuw Amerongen *et al.*, 2003). Similarly, Shrm2 knockdown in HUVEC cells results in significant reduction of migration as assayed in a Boyden chamber (Figure 4D).

To better understand how Shrm2 may regulate migration, we evaluated the localization of Shrm2 during wounding. Wounded monolayers of C166 cells were fixed and stained to detect Shrm2 and actin (Figure 4E). At 2 h after wounding, Shrm2 can be found on thick F-actin cables at the leading edge. This structure is hypothesized to resemble a purse string, drawing cells into the wound (Tamada *et al.*, 2007). At this time, Rock is also found at the leading edge. Again, this localization is dependent upon Shrm2, as Shrm2 knockdown abolishes Rock localization at the leading edge (Figure 4, F and G). At 12 h after wounding, Shrm2 is diffusely localized at the leading edge and by 24 h is ultimately lost from the leading edge as cells completely detach from the monolayer. Because these detached cells have little Shrm2 protein, it seems logical that reduction of Shrm2 promotes migration into the wound.

To better understand the consequence of long-term loss of Shrm2 function in endothelial cells, we generated a stable C166 cell line expressing a Shrm2-specific shRNA from the pSuper-GFPneo^r vector. Stable expression of the shRNA leads to apparent 100% knockdown as Shrm2 protein is undetectable via Western blot (Figure 5A). Analysis of the effect of stable Shrm2 knockdown indicates a change in morphogenesis: a loss of dense peripheral actin bundles observed in control cells and an increase in filopodial extensions (Figure 5, C and D). Control cells are often found clustered and adherent to one another, while shShrm2 cells fail to cluster or form stable cell–cell contacts. shShrm2 C166 cells contain fewer central FAs but larger peripheral FAs (Figure 5, E–H). The loss of central FAs has also been observed in mouse embryonic fibroblasts treated with Y27632, highlighting the importance of Rock-mediated contractility in FA regulation (Pasapera *et al.*, 2010). As expected, expression of shShrm2 further enhances migration in a Boyden chamber compared with control or transient siRNA knockdown (Figure 5B). Because shShrm2 cells fail to adhere to one another and form a monolayer, wound healing was assessed by mixing vector control (pSuper) or stable shShrm2 cells—both green fluorescent protein (GFP) positive—with wild-type C166 cells. Monolayers were then wounded, and the migration of control or shShrm2 cells into the wound was assayed 30 min later. In controls, the GFP-positive cells are still integrated into the monolayer (arrow) and possess robust actin belts at the leading edge (arrowhead) (Figure 5I). In contrast shShrm2 cells fail to adhere to the monolayer and after only 30 min have started to migrate into the wound, past the actin belt (Figure 5J). Presumably due to the increase in migration and loss of cellular adhesion, these cells fail to undergo angiogenesis on matrigel (unpublished data). On the basis of these results and those presented above, we predict that loss of signaling via the Shrm2–Rock complex reduces the degree of cortical actomyosin contractility, which in turn promotes the migration of the C166 cells.

DISCUSSION

The actin and Rock binding protein Shrm2 is expressed within the mouse vasculature during development. Here we demonstrate a role for Shrm2 in the regulation of endothelial morphology, as knockdown of Shrm2 in C166 endothelial cells, HUVECs, and differentiated mES cells results in increased endothelial branching. We propose the following role for Shrm2 in the regulation of angiogenesis during embryonic development (Figure 6). Through the actin binding SD1, and perhaps through the serine/proline-rich region (SPR) responsible for interaction with ZO1, Shrm2 localizes to cortical actin (Dietz *et al.*, 2006; Etournay *et al.*, 2007). Through the SD2 domain, Shrm2 recruits Rock, which is predicted to phosphorylate the myosin regulatory light chain and activate myosin II, thereby establishing a cortical, contractile network. As indicated by changes in stress fiber organization, pFAK levels, and FA architecture in Shrm2 knockdown cells, Shrm2-dependent contractility can influence additional cellular processes including actin organization, cellular migration, and endothelial branching, ultimately affecting the morphology of the vascular network.

It is currently unknown how the Shrm2–Rock complex might be regulated. While many processes that require Rock also require the activity of Rho, previous studies suggest that the ability of Shrm proteins to control contraction is independent of RhoA (Haigo *et al.*, 2003; Hildebrand, 2005). Therefore it is possible that Shrm2 binding to Rock serves to both localize and activate the kinase. We suggest that one critical step in regulation is correct subcellular distribution. This is evidenced by previous observations that Shrm2, Shrm3, and Shrm4 have different subcellular localization and cause different

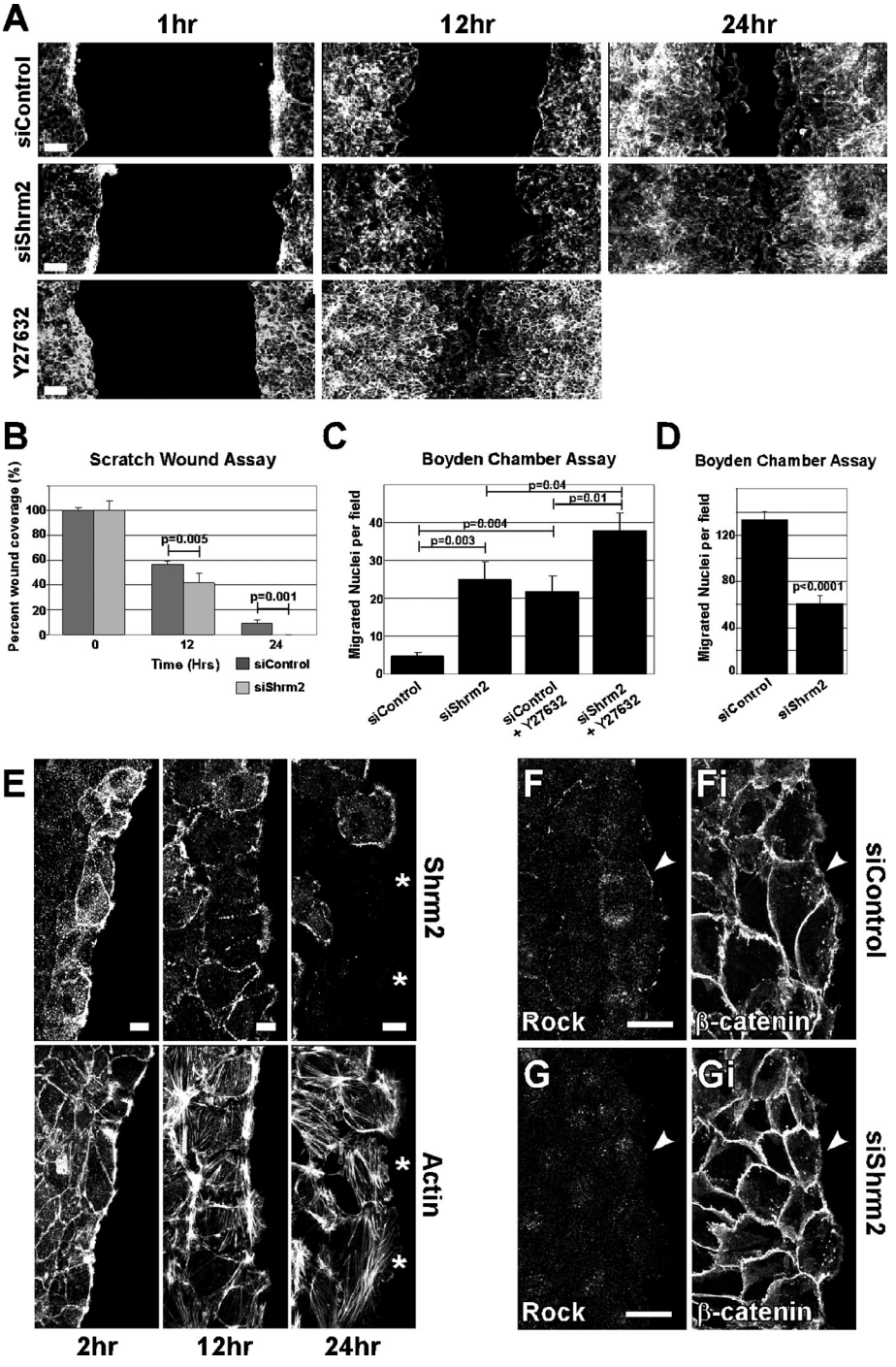

FIGURE 4: Transient knockdown of Shrm2 regulates endothelial migration. (A) siControl, siShrm2, or untreated cells with Y27632 were subjected to a scratch wound assay and were stained with phalloidin at 1, 12, and 24 h postscratch. (B) Quantification of a scratch wound assay from live C166 cells treated with siControl or siShrm2, represented by the mean percentage of wound closure ± SD (n = 5). (C) Migration of siControl and siShrm2 C166 cells in the presence or absence of Y27632 was assessed with a Boyden chamber. (D) Migration of siControl and siShrm2-treated HUVEC cells in a Boyden chamber. The number of migrated nuclei is represented by the mean ± SEM (n = 6) in C and D. (E) Untreated C166 cells were scratch wounded and stained for Shrm2 and actin at 2, 12, and 24 h postscratch. Asterisks indicate cells that have detached from the epithelial sheet and have lost Shrm2 expression. (F and G) At 2 h after scratch wounding C166 cells, Rock1 localizes to the leading edge of siControl (F) but not siShrm2 (G) C166 cells. Immunostaining for β-catenin (Ei and Fi). Scale bars = 100 μm in A; 25 μm in B, E, and F.

phenotypes when expressed in cells despite the fact that they all have the capacity to trigger myosin II–dependent changes in cell shape (Dietz *et al.*, 2006). While actin binding is a critical aspect of the correct localization of Shrm proteins, other sequences in the N-terminal region, including the PDZ and SPR domains, likely contribute to their functions. The SPR domains of Shrm2 and Shrm3 appear to participate in direct interactions with ZO1 and POSH, respectively, and their SH3 domains are required for these interactions (Etournay *et al.*, 2007; Taylor *et al.*, 2008). Through an interaction with POSH, Shrm3 negatively regulates neurite outgrowth in a Rock-dependent manner (Taylor *et al.*, 2008). It is intriguing that both Shrm2 and Shrm3 can negatively regulate two physiologically different branching processes. While the Shroom family of proteins has the capacity to alter morphology through an interaction with Rock, Shrm2 is not able to reproduce the apical constriction of MDCK cells caused by Shrm3 expression (Dietz *et al.*, 2006). It is therefore apparent that through tissue-specific expression and unique localization mechanisms, the Shroom family can alter morphology in similar yet unique ways. It has been proposed that the ZO1/Shrm2 interaction helps facilitate tight junction stability (Etournay *et al.*, 2007). However, we see no changes in ZO1 localization following Shrm2 knockdown, and siShrm2-treated cells can readily form tight junctions after passage to a new plate (unpublished data). Reciprocally, ZO1 knockdown has no affect on Shrm2 localization (Supplemental Figure S4), suggesting that Shrm2 does not localize via ZO1 alone. Additional experiments will be necessary to elucidate the relationship between ZO1, Shrm2, and the establishment of cortical contractility.

The Shrm family of proteins is characterized by its evolutionarily conserved Rock binding domain, SD2 (Dietz *et al.*, 2006; Nishimura and Takeichi, 2008). In this study we demonstrate an interaction between the SD2 domain of Shrm2 and Rock. We also show that Shrm2 is required for localization of Rock at endothelial tight junctions and that Shrm2-deficient C166 cells are more sensitive to Rock inhibition, decreasing contractility and increasing migration. These data support a role for Shrm2 in the localization of Rock and establishment of endothelial contractility, the loss of which results in increased angiogenesis. Interestingly, near complete reduction of Shrm2 through stable expression of shRNA or incubation with a Rock inhibitor completely abolishes matrigel angiogenesis of C166 cells (unpublished data). Because transient knockdown with Shrm2 siRNA leads to an increase in branching, we propose that a Shrm2/Rock-dependent contractility threshold exists such that slight reductions in contractility increase branching, whereas significant reduction abolishes angiogenesis. It is also likely that Shrm2 mediates only a

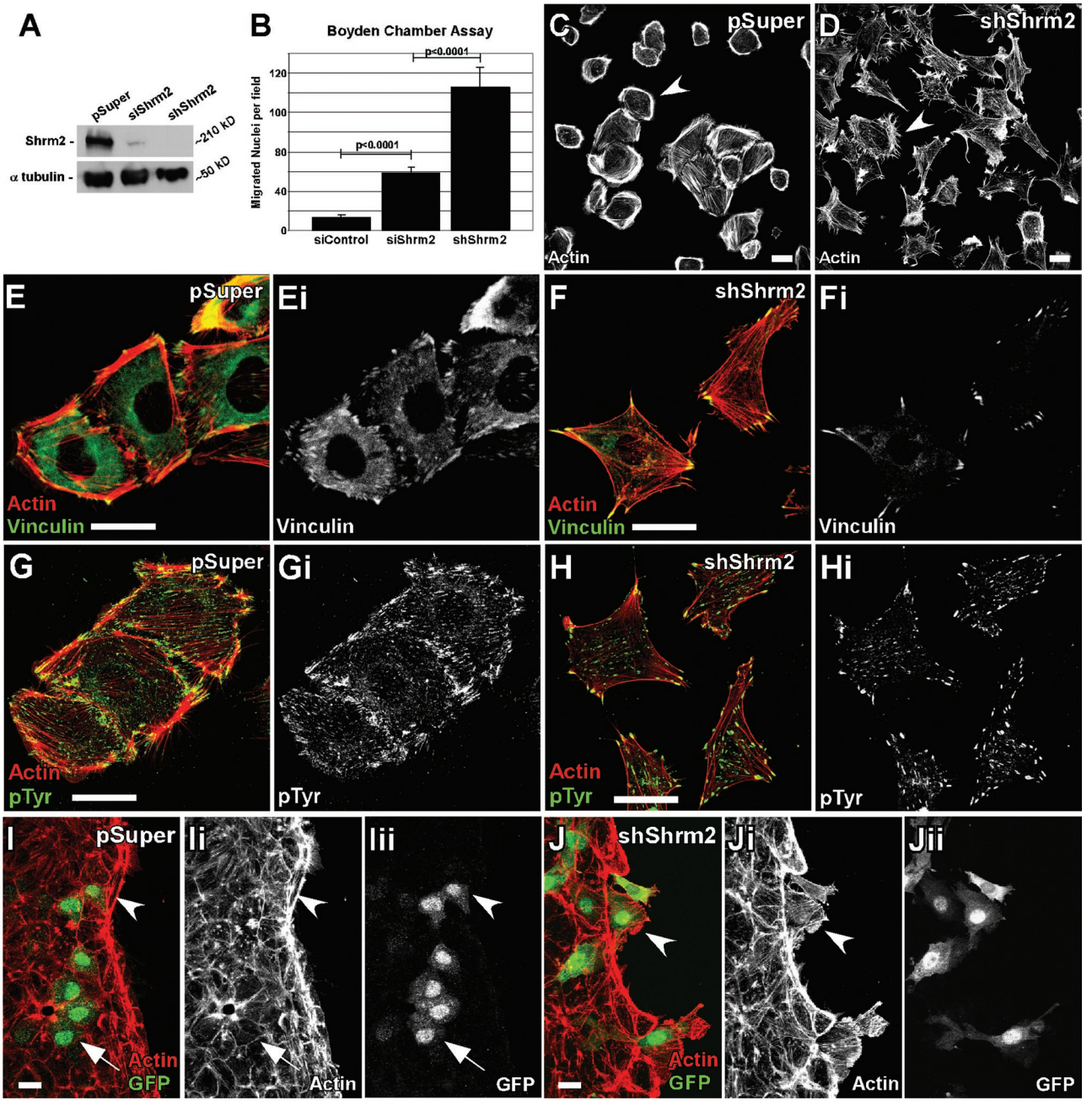

FIGURE 5: Stable expression of shShrm2 changes endothelial morphology and enhances migration. (A) Western blot of transient siShrm2, stable shShrm2, or stable vector control (pSuper) C166 cells for Shrm2. α-Tubulin was used as a loading control. (B) Quantification of Boyden chamber migration for siControl, siShrm2, or shShrm2 C166 cells. The number of migrated nuclei is represented by the mean ± SEM (n = 6). (C and D) pSuper (C) or shShrm2 (D) C166 cells were allowed to spread on fibronectin-coated coverslips for 4 h and were immunostained for actin. Arrowheads indicate differences in cortical actin. (E–H) pSuper (E and G) or shShrm2 (F and H) C166 cells were immunostained for vinculin (E and F) or phospho-tyrosine (G and H) to visualize focal adhesions. (I and J) pSuper (I) or shShrm2 (J) C166 cells (indicated by GFP) were mixed with parent C166 cells and wounded. Cells were allowed to migrate for 30 min and were then stained for GFP and actin. Arrows indicate stable junctions formed between pSuper and parent C166 cells. Arrowheads indicate pSuper cells that contribute to the actin belt or shShrm2 cells that migrate quickly into the wound past the actin belt. Scale bars = 25 μm.

subset of Rock activity essential for angiogenesis, as Rock activation and localization can be regulated by other factors such as RhoA, lipids, and dynamin I (Tumusiime *et al.*, 2009). And while Shrm2 can interact with both Rock1 and Rock2, it remains to be determined how the different Rock isoforms impact angiogenesis.

Conflicting reports for the role of Rock in angiogenesis have been well documented (reviewed in van Nieuw Amerongen and van Hinsbergh, 2009). Many of these studies utilize general Rock inhibitors that present the possibility of off-target effects. Here we suggest that Shrm2 is involved in a specific aspect of Rock activity

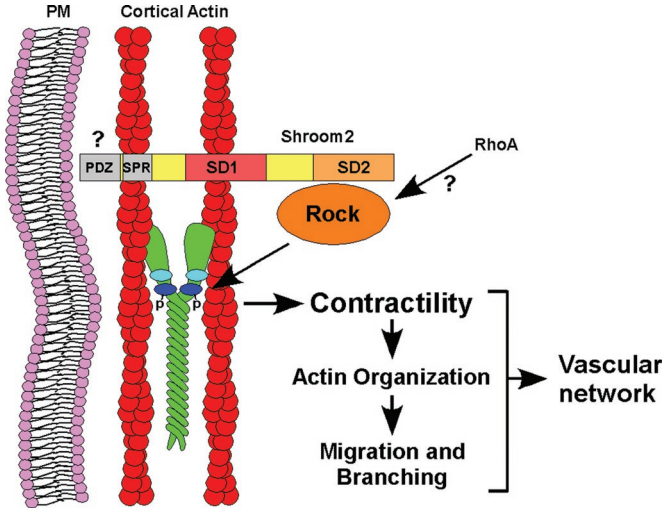

FIGURE 6: Model of Shrm2 function in endothelial cells. Shrm2 localization to cortical actin is mediated, in part, by the actin binding domain SD1. The Shrm2 SD2 domain recruits Rock to cortical actin, where it activates the myosin regulatory light chain of myosin II, establishing cellular contractility. Changes in contractility are thought to influence cellular migration and branching through changes in actin organization, which ultimately impacts vascular morphology.

during angiogenesis, specifically the cortical recruitment of Rock and activation of downstream myosin II activity. The unique ability of Shrm2 to recruit Rock to a specific subcellular location suggests that Shrm2 may provide a novel way to target specific Rock-dependent processes while leaving others unaffected. Several studies of the role of Rock in the vasculature support our findings and predictions. Rock RNA interference (RNAi) increases endothelial sprouting in both HUVEC spheroid culture and murine retinas (Kroll *et al.*, 2009). It has also been demonstrated that local loss of myosin II cortical contractility results in filopodia-like extensions in endothelial cells (Fischer *et al.*, 2009). Additional studies suggest that Rock-dependent actomyosin contractility can lead to VE-cadherin accumulation at endothelial cell–cell junctions promoting cell adhesion, inhibition of VEGFR2, and vessel quiescence. Perturbation of this system through Rock inhibition or knockdown of VE-cadherin leads to an increase in vessel sprouting (Abraham *et al.*, 2009). The phenotypic outcome of Shrm2 knockdown is reminiscent of that observed following VE-cadherin knockdown such that both lead to increased cord formation and decreased MLC2 phosphorylation (Abraham *et al.*, 2009). Interestingly, following transient knockdown of Shrm2 in C166 cells, we do not see changes in cell–cell adhesion, as measured by β-catenin and ZO1 staining. Therefore it appears that the ability of Shrm2 to control contractility and subsequent endothelial morphogenesis may be independent of cadherin-mediated adhesion. However, it should also be noted that C166 cells are devoid of VE-cadherin and thus may use another cadherin for cell–cell interactions that does not function in a manner analogous to that of VE-cadherin (unpublished data). Another distinction between these experimental systems is that C166 cells do not require the addition of VEGF, suggesting that the relationship between VEGF, VE-cadherin, and morphogenesis has been uncoupled in these cells. This suggests that there may be different, independent pathways working to promote the formation of peripheral actomyosin networks that control the angiogenic behavior of endothelial cells. Alternatively, we could predict that these two pathways may intersect at the level of the cortical actin network in adherent cells in order to reinforce one another and that both are required to maintain cortical contractility and restrict the migratory and branching potential of endothelial cells. The link between cadherin signaling and Shrm2 will be an interesting and valuable avenue of investigation.

In conclusion, we show that Shrm2 is expressed in the developing vasculature and is required for proper angiogenesis. Reducing Shrm2 levels with Shrm2 RNAi decreases endothelial contractility and leads to increased endothelial sprouting. Because Shrm2 physically interacts with Rock and Shrm2-deficient cells are more sensitive to Rock inhibition, we propose that Shrm2 and Rock interact to regulate cellular contractility, which in turn controls cytoskeletal architecture, motility, and, ultimately, endothelial angiogenesis.

MATERIALS AND METHODS

Cell culture and RNAi

C166 cells were maintained at 37°C, 5% CO_2 in DMEM supplemented with 10% fetal bovine serum (FBS), pen/strep, and L-glutamine. Pooled HUVECs were purchased from ATCC (Manassas, VA) and cultured in Vascular Cell Basal media (ATCC) supplemented with Endothelial Cell Growth Kit (ATCC). ON-TARGETplus siRNAs were ordered from Dharmacon (Lafayette, CO) and were tested for knockdown efficiency by immunofluorescence analysis and Western blotting. The following two siRNA duplexes were most efficient: mShrm2–7 sense sequence: AGUCAAGAUUGGCGAGA; mShrm2–8 sense sequence: GGAUAAUGUUGAACCCAAA. The ON-TARGETplus SMARTpool for hShrm2 was used in HUVEC cells. ON-TARGETplus nontargeting siRNA #1 was used as a control. C166 cells were transfected in suspension with 100 nM siRNA using Lipofectamine 2000. Adherent HUVEC cells were transfected with 100 nM siRNA using Dharmafect #1 (Dharmacon). Cells were allowed to grow for 72 h before use. Inducible Shrm2-expressing cells were made by transfecting T23 MDCK cells with pTRE2-hygro containing a full-length Shrm2 cDNA. Cells were selected in Eagle's minimum essential medium/10% FBS containing 200 μg/ml hygromycin and 40 ng/ml doxycycline for 10 d. Individual clones were isolated, expanded, and tested by Western blotting for inducible expression of Shrm2 protein.

Immunofluorescence

Cells were grown on fibronectin-coated coverslips, fixed in either 4% paraformaldehyde (PFA) or −20° MeOH, and stained as previously described (Hildebrand, 2005). Shrm2 antibodies were prepared as previously described (Dietz *et al.*, 2006). Additional antibodies were as follows: PECAM, E-cadherin (BD Biosciences, Franklin Lakes, NJ); ZO1 (Santa Cruz Biotechnology, Santa Cruz, CA); α-tubulin (Sigma-Aldrich, St. Louis, MO); Rock1, pMLC2–Ser-19, ppMLC2–Thr-18/Ser-19, p-cofilin, and pFAK–Tyr-397 (Cell Signaling, Danvers, MA); Rock2 (Bethyl Labs, Montgomery, TX); p-MYPT (Millipore, Temecula, CA); and GFP, TO-PRO-3, goat anti–mouse, goat anti–rat, or goat anti–rabbit secondary antibodies conjugated to Alexa-488 or Alexa-568 (Invitrogen, Carlsbad, CA).

Matrigel angiogenesis assay

C166 or HUVEC cells were used 72 h after transfection with siRNA. A thin layer of matrigel (BD Biosciences, Franklin Lakes, NJ) was spread onto six-well plates and allowed to harden. Then 2×10^6 C166 cells or 5×10^5 HUVECs were placed in each well with complete media. For the C166 cells, multicellular chords form after 24 h (Supplemental Figure S2, A and B) and after ~5 d resolve into a thinner network with no change in the branching architecture (Figure 1, F–H). When fewer C166 cells are plated (1.2×10^6), short cords emerge but fail to form an interconnected network (Supplemental Figure S2A). Cells were photographed with an Olympus MVX10.

Sprouting angiogenesis assay

C166 cells were used 48 h after transfection with siRNA. Spheroids of a similar cell number were formed by resuspending 400 C166 cells/well in Methocel media (20% Methocel, 80% culture media) in a nontissue culture–treated 96-well plate (Thermo Fisher Scientific, Pittsburgh, PA), which was placed at 37° O/N. Spheroids were harvested and resuspended in DMEM with 20% FBS and 30 ng/ml rmVEGF (R&D Systems, Minneapolis, MN). Then 250 µl spheroids was mixed with 250 µl collagen (Millipore, Temecula, CA), neutralized with NaOH, and plated in a 24-well plate (BD Falcon, Franklin Lakes, NJ). Collagen gels were given 30 min to polymerize at 37° and were then overlaid with media + 300 ng/ml rmVEGF. Sprouts were photographed after 48 h.

Vasculogenesis assay

shRNA oligos corresponding to mShrm2–7 and mShrm2–8 siRNAs (Oligoengine, Seattle, WA) were cloned into the pSuper-gfpneo^r vector (Oligoengine). The plasmid was linearized and electroporated into mouse ES cells (cell line Ak7, a gift from Philippe Soriano). For generation of stable C166 cells, uncut plasmid was transfected and cells were selected for G418 resistance. Drug-resistant cells were pooled and tested for GFP fluorescence and Shrm2 knockdown. ES cells cultured in DMEM with L-glutamine, Pen/Strep, 20% ES certified FBS (Thermo Scientific Hyclone, Logan, UT), 0.1 mM NEAA (Life Technologies, Carlsbad, CA), and 0.1 mM BME were grown on a layer of SNL fibroblasts (a gift from Philippe Soriano) that had been mitotically inactivated with mitomycin C (Sigma-Aldrich, St. Louis, MO). SNLs were grown on collagen-coated tissue culture plates. After 24 h, positive transformants were selected in 300 µg/ml G418 for 9–11 d, changing media every day. GFP-positive colonies were selected for expansion and were verified for Shrm2 KD via immunostaining and Western blot. Differentiation of ES cells into endothelial vessels was performed as described by Kappas and Bautch (2007). Briefly, older, more flattened ES colonies were chosen for differentiation. ES colonies were detached with Dispase and cultured on bacteriological Petri dishes for 3 d. Resultant embryoid bodies were allowed to reattach on fibronectin-coated coverslips in differentiation media: DMEM + 20% ES certified FBS, Pen/Strep, L-glutamine, 300 µg/ml G418, and 75 µm monothioglycerol. After 8–10 d, endothelial vessels were examined by immunostaining with a PECAM antibody.

Collagen gel contraction

The 1-mg/ml gels were prepared by diluting collagen with media, neutralizing with NaOH, and plating 500 µl/well in a 24-well plate. C166 cells were used 48 h after siRNA transfection, and 2.5×10^5 cells/well in 500 µl media were placed in the well. After 24 h, the collagen gel was detached with a yellow tip pipette and photographed after 6 h.

Western blotting

For Western blots of Shrm2 and loading controls, cells were lysed in radio immunoprecipitation assay buffer, separated on 10% polyacrylamide gels, transferred to nitrocellulose, and subjected to immunoblotting. For Western blots of phosphoproteins, cells were lysed and resuspended in sample buffer (62.5 mM Tris-HCL, pH 6.8, 2% SDS, 10% glycerol, 50 mM dithiothreitol).

In vitro binding

mShrm2 cDNA corresponding to amino acids (aa) 1286–1479 (SD2 domain) was cloned into the pET151 vector, which contains a His tag. hRock1 cDNA corresponding to amino acids 681–942 (SBD) was cloned into the pRSF vector. Both vectors were transformed into BL21 cells. Expression was induced with 0.5 mM isopropyl β-D-1-thiogalactopyranoside (IPTG) for 1 h before lysing via sonication. His-tagged SD2 was bound onto Ni-NTA resin, eluted with sample buffer, separated on a polyacrylamide gel, and Coomassie stained.

GST pull down

mShrm2 cDNA corresponding to aa 1068–1480 was cloned into pGEX-2T, and hRock1 cDNA corresponding to aa 593–1062 was cloned into pGEX-3X and transformed individually into RIPL cells. After IPTG induction and lysing, GST-mShrm2-SD2, GST-hRock1-SBD, and GST alone were bound to glutathione Sepharose beads (GE Healthcare, Piscataway, NJ) and then incubated with cell lysate at 4°C for 2 h. C166 or T23:TRE Shrm2 cells were lysed via sonication in NETN buffer (20 mM Tris pH8.0, 100 mM NaCl, 1 mM EDTA, 0.5% NP-40, and 1:100 protease and phosphatase inhibitor cocktails). After incubation, glutathione Sepharose was washed four times in NETN buffer, resuspended in SDS sample buffer, and analyzed via Western blot.

Scratch wound assay

For this assay, 6×10^5 C166 cells were transfected in suspension and plated on fibronectin-coated coverslips in a six-well plate. After 72 h, cells were scratched with a yellow tip pipette to generate consistently sized wounds. Representative wounds were fixed in PFA and stained with phalloidin. To quantify migration, live cells at the same wound site were photographed at 1, 12, and 24 h postscratch and quantified.

Boyden chamber assay

At 72 h after transfection with siRNA, 1×10^5 C166 cells or 7.5×10^4 HUVECs were plated in the upper chamber of a fibronectin-coated, 8.0 µm polycarbonate, 24-well transwell insert (Costar, Corning, Lowell, MA). Cells were allowed to migrate for 4 h. The top chamber was scraped with a Q-tip, and the bottom cells were fixed in PFA, stained with phalloidin and TO-PRO, and photographed. Nuclei were counted from three random fields of view of two independent experiments.

Statistics

All measures of significance were determined by one-tailed, unpaired *t* test.

ACKNOWLEDGMENTS

We thank members from the labs of J. Hildebrand, D. Chapman, and B. Roman for useful discussion during the course of this work and William Saunders for live cell imaging advice. J.D.H. was funded by the National Institute of General Medical Sciences.

REFERENCES

Abraham S, Yeo M, Montero-Balaguer M, Paterson H, Dejana E, Marshall CJ, Mavria G (2009). VE-cadherin-mediated cell-cell interaction suppresses sprouting via signaling to MLC2 phosphorylation. Curr Biol 19, 668–674.

Amano M, Ito M, Kimura K, Fukata Y, Chihara K, Nakano T, Matsuura Y, Kaibuchi K (1996). Phosphorylation and activation of myosin by Rho-associated kinase (Rho-kinase). J Biol Chem 271, 20246–20249.

Bolinger C, Zasadil L, Rizaldy R, Hildebrand JD (2010). Specific isoforms of *Drosophila* shroom define spatial requirements for the induction of apical constriction. Dev Dyn 239, 2078–2093.

Bryan BA, Dennstedt E, Mitchell DC, Walshe TE, Noma K, Loureiro R, Saint-Geniez M, Campaigniac JP, Liao JK, D'Amore PA (2010). RhoA/ROCK signaling is essential for multiple aspects of VEGF-mediated angiogenesis. FASEB J 24, 3186–3195.

Chung MI, Nascone-Yoder NM, Grover SA, Drysdale TA, Wallingford JB (2010). Direct activation of Shroom3 transcription by Pitx proteins drives

epithelial morphogenesis in the developing gut. Development 137, 1339–1349.
De Smet F, Segura I, De Bock K, Hohensinner PJ, Carmeliet P (2009). Mechanisms of vessel branching: filopodia on endothelial tip cells lead the way. Arterioscler Thromb Vasc Biol 29, 639–649.
Dietz ML, Bernaciak TM, Vendetti F, Kielec JM, Hildebrand JD (2006). Differential actin-dependent localization modulates the evolutionarily conserved activity of Shroom family proteins. J Biol Chem 281, 20542–20554.
Etournay R, Zwaenepoel I, Perfettini I, Legrain P, Petit C, El-Amraoui A (2007). Shroom2, a myosin-VIIa- and actin-binding protein, directly interacts with ZO-1 at tight junctions. J Cell Sci 120, 2838–2850.
Fairbank PD, Lee C, Ellis A, Hildebrand JD, Gross JM, Wallingford JB (2006). Shroom2 (APXL) regulates melanosome biogenesis and localization in the retinal pigment epithelium. Development 133, 4109–4118.
Fischer RS, Gardel M, Ma X, Adelstein RS, Waterman CM (2009). Local cortical tension by myosin II guides 3D endothelial cell branching. Curr Biol 19, 260–265.
Haigo SL, Hildebrand JD, Harland RM, Wallingford JB (2003). Shroom induces apical constriction and is required for hingepoint formation during neural tube closure. Curr Biol 13, 2125–2137.
Hildebrand JD (2005). Shroom regulates epithelial cell shape via the apical positioning of an actomyosin network. J Cell Sci 118, 5191–5203.
Hildebrand JD, Soriano P (1999). Shroom, a PDZ domain–containing actin-binding protein, is required for neural tube morphogenesis in mice. Cell 99, 485–497.
Ishizaki T, Naito M, Fujisawa K, Maekawa M, Watanabe N, Saito Y, Narumiya S (1997). p160ROCK, a Rho-associated coiled-coil forming protein kinase, works downstream of Rho and induces focal adhesions. FEBS Lett 404, 118–124.
Kappas NC, Bautch VL (2007). Maintenance and in vitro differentiation of mouse embryonic stem cells to form blood vessels. Curr Protoc Cell Biol 34, 23.3.1–23.3.20.
Kimura K *et al.* (1996). Regulation of myosin phosphatase by Rho and Rho-associated kinase (Rho-kinase). Science 273, 245–248.
Kroll J, Epting D, Kern K, Dietz CT, Feng Y, Hammes HP, Wieland T, Augustin HG (2009). Inhibition of Rho-dependent kinases ROCK I/II activates VEGF-driven retinal neovascularization and sprouting angiogenesis. Am J Physiol Heart Circ Physiol 296, H893–H899.
Le Boeuf F, Houle F, Sussman M, Huot J (2006). Phosphorylation of focal adhesion kinase (FAK) on Ser732 is induced by rho-dependent kinase and is essential for proline-rich tyrosine kinase-2–mediated phosphorylation of FAK on Tyr407 in response to vascular endothelial growth factor. Mol Biol Cell 17, 3508–3520.
Lee C, Le MP, Wallingford JB (2009). The shroom family proteins play broad roles in the morphogenesis of thickened epithelial sheets. Dev Dyn 238, 1480–1491.
Lee C, Scherr HM, Wallingford JB (2007). Shroom family proteins regulate γ-tubulin distribution and microtubule architecture during epithelial cell shape change. Development 134, 1431–1441.
Maekawa M, Ishizaki T, Boku S, Watanabe N, Fujita A, Iwamatsu A, Obinata T, Ohashi K, Mizuno K, Narumiya S (1999). Signaling from Rho to the actin cytoskeleton through protein kinases ROCK and LIM-kinase. Science 285, 895–898.
Mavria G, Vercoulen Y, Yeo M, Paterson H, Karasarides M, Marais R, Bird D, Marshall CJ (2006). ERK-MAPK signaling opposes Rho-kinase to promote endothelial cell survival and sprouting during angiogenesis. Cancer Cell 9, 33–44.
Millán J, Cain RJ, Reglero-Real N, Bigarella C, Marcos-Ramiro B, Fernández-Martín L, Correas I, Ridley AJ (2010). Adherens junctions connect stress fibres between adjacent endothelial cells. BMC Biol 8, 11.
Nishimura T, Takeichi M (2008). Shroom3-mediated recruitment of Rho kinases to the apical cell junctions regulates epithelial and neuroepithelial planar remodeling. Development 135, 1493–1502.
Pasapera AM, Schneider IC, Rericha E, Schlaepfer DD, Waterman CM (2010). Myosin II activity regulates vinculin recruitment to focal adhesions through FAK-mediated paxillin phosphorylation. J Cell Biol 188, 877–890.
Riento K, Ridley AJ (2003). Rocks: multifunctional kinases in cell behaviour. Nat Rev Mol Cell Biol 4, 446–456.
Tamada M, Perez TD, Nelson WJ, Sheetz MP (2007). Two distinct modes of myosin assembly and dynamics during epithelial wound closure. J Cell Biol 176, 27–33.
Taylor J, Chung KH, Figueroa C, Zurawski J, Dickson HM, Brace EJ, Avery AW, Turner DL, Vojtek AB (2008). The scaffold protein POSH regulates axon outgrowth. Mol Biol Cell 19, 5181–5192.
Tumusiime S, Rana MK, Kher SS, Kurella VB, Williams KA, Guidry JJ, Worthylake DK, Worthylake RA (2009). Regulation of ROCKII by localization to membrane compartments and binding to DynaminI. Biochem Biophys Res Commun 381, 393–396.
Uehata M *et al.* (1997). Calcium sensitization of smooth muscle mediated by a Rho-associated protein kinase in hypertension. Nature 389, 990–994.
van Nieuw Amerongen GP, Koolwijk P, Versteilen A, van Hinsbergh VW (2003). Involvement of RhoA/Rho kinase signaling in VEGF-induced endothelial cell migration and angiogenesis in vitro. Arterioscler Thromb Vasc Biol 23, 211–217.
van Nieuw Amerongen GP, van Hinsbergh VW (2009). Role of ROCK I/II in vascular branching. Am J Physiol Heart Circ Physiol 296, H903–H905.
Wang SJ, Greer P, Auerbach R (1996). Isolation and propagation of yolk-sac-derived endothelial cells from a hypervascular transgenic mouse expressing a gain-of-function fps/fes proto-oncogene. In Vitro Cell Dev Biol Anim 32, 292–299.
Watanabe T, Hosoya H, Yonemura S (2007). Regulation of myosin II dynamics by phosphorylation and dephosphorylation of its light chain in epithelial cells. Mol Biol Cell 18, 605–616.
Zhou X, Stuart A, Dettin LE, Rodriguez G, Hoel B, Gallicano GI (2004). Desmoplakin is required for microvascular tube formation in culture. J Cell Sci 117, 3129–3140.